

Stardust: Compiling Sparse Tensor Algebra to a Reconfigurable Dataflow Architecture

Olivia Hsu
Stanford University
Stanford, CA, USA
owhsu@stanford.edu

Alexander Rucker
Stanford University
Stanford, CA, USA
acrucker@stanford.edu

Tian Zhao
Stanford University
Stanford, CA, USA
tianzhao@stanford.edu

Kunle Olukotun
Stanford University
Stanford, CA, USA
kunle@stanford.edu

Fredrik Kjolstad
Stanford University
Stanford, CA, USA
kjolstad@stanford.edu

Abstract

We introduce Stardust, a compiler that compiles sparse tensor algebra to reconfigurable dataflow architectures (RDAs). Stardust introduces new user-provided data representation and scheduling language constructs for mapping to resource-constrained accelerated architectures. Stardust uses the information provided by these constructs to determine on-chip memory placement and to lower to the Capstan RDA through a parallel-patterns rewrite system that targets the Spatial programming model. The Stardust compiler is implemented as a new compilation path inside the TACO open-source system. Using cycle-accurate simulation, we demonstrate that Stardust can generate more Capstan tensor operations than its authors had implemented and that it results in 138× better performance than generated CPU kernels and 41× better performance than generated GPU kernels.

Keywords: Sparse Tensor Algebra, Compilation, Scheduling Language, RDA, Parallel Patterns, Accelerators

1 Introduction

Sparse tensor algebra (including linear algebra) is used in many applications, including data analytics [5], computational science [4], and machine learning [1]. To accelerate sparse computation, hardware designers are developing specialized domain-specific accelerators [9, 13, 25].

Tensor algebra can be used to express a variety of computations. However, only a few functions, such as dense matrix multiplication and sparse matrix-vector multiplication, are used widely enough to warrant single-function hardware. This leaves a long tail of important tensor computations for which we cannot afford to build single-function hardware, but which would still benefit from performance and energy efficiency improvements beyond what is possible with CPUs and GPUs. Examples include tensor factorization in data analytics [5], tensor contractions in computational chemistry [11], and graph analytics expressed as linear algebra [22]. Kernel fusion enabled by compilers boosts arithmetic intensity [30, 42] and avoids unnecessary work [19].

To address the long tail of sparse functions that need to be accelerated, one promising approach is reconfigurable dataflow architectures (RDAs) with support for sparse operations [14, 30]. RDAs provide general hardware for combining sparse data streams and for storing sparse temporary data structures on chip. They can be used to efficiently compute many different sparse linear and tensor algebra expressions. But to date, these architectures have only been programmed directly at the level of their sparse data combiners and physical memories. This means that programming them is not amenable to data scientists and machine learning software developers. Whereas to make RDAs much more accessible, we propose compiling to them directly from sparse tensor algebra expressions, along with a provided schedule, through a library API.

The challenge in compiling to sparse RDAs is managing their memories and controlling the combining of sparse streams of tensor coordinate-value pairs. On CPUs and GPUs, the von Neumann architecture separates control logic from memories and presents the programmer with a convenient pull model—when you need data, you ask for it. But on RDAs the control logic is attached to memories in a push model of computation, where programmers explicitly manage data movement throughout the memory hierarchy. These challenges make RDAs harder to program than CPUs and GPUs, which is exacerbated by the complexity of sparse tensor algebra kernels.

Following Halide [28] and TACO [31], we separate algorithms from schedules. And, like TACO, we further separate data representations [18]. This design lets end users of tensor algebra focus on their application logic, using intuitive linear and tensor algebra expressions exposed as a library. These expressions can then be mapped to a CPU or, using the scheduling and data representation languages, to a dataflow architecture. Thus, end users and performance engineers can work separately. The experience from Halide [28] has been that a clean scheduling language facilitates auto-scheduling research [2, 3, 24, 29] and lets performance experts tune code beyond the capabilities of current auto-scheduling systems.

In this paper, we describe how to compile arbitrary sparse tensor algebra expressions to Capstan [30], a recently published RDA. The key insight is to use separate languages to describe the tensor expression, the data representations and their placement on the RDA, and the mapping of the sparse iteration space of a tensor expression to sparse hardware.

Contributions. Stardust is the first system that compiles sparse tensor algebra to a sparse RDA. Our contributions are:

- a data representation language that can express accelerator tensor placement,
- a scheduling language that can express how portions of a (potentially transformed) sparse iteration space should be mapped to sparse accelerators,
- an algorithm that binds descriptions of data structures to specific physical memories, and
- a lowering rewrite system that maps sparse tensor algebra expressions to the declarative-sparse Spatial programming model for RDAs.

We implemented these concepts as a new compilation path in the open source TACO system [18], extending its data representation and scheduling languages to target dataflow hardware, as shown in Figure 1. We then use Stardust to compile a previously used benchmark set [18] to the Capstan RDA [30]. The data representation and scheduling languages in Stardust are sufficient to express optimized algorithms that outperform CPUs by 138 \times and GPUs by 41 \times . Furthermore, the mapping languages enable new algorithms beyond those previously mapped to Capstan [30], demonstrating that the separation of algorithm, data representation, and scheduling provides a viable path for compilation to domain-specific architectures.

2 Overview

Stardust takes three inputs: a tensor algebra expression, formats [8], and a schedule [31]. These combine to produce an algorithm expressed in the *concrete index notation* (CIN) intermediate representation (IR) of Kjolstad et al. [17]. Figure 1 shows the relationship between our contributions (orange) and prior work on the TACO compiler (blue). Unlike TACO, which generates C++ [18] and CUDA [31] to target von Neumann machines, Stardust generates Spatial code [20] with parallel patterns to target a sparse RDA [30].

Domain-specific accelerators are by their nature more specialized than CPUs. And, although Capstan is more flexible than fixed-function hardware, it is still a specialized machine. To target specialized hardware, a user writes a schedule that reorganizes the computation until a sub-computation is exposed that maps directly onto the hardware. Although TACO cannot map computation to specialized hardware, Stardust inherits its powerful sparse transformation framework.

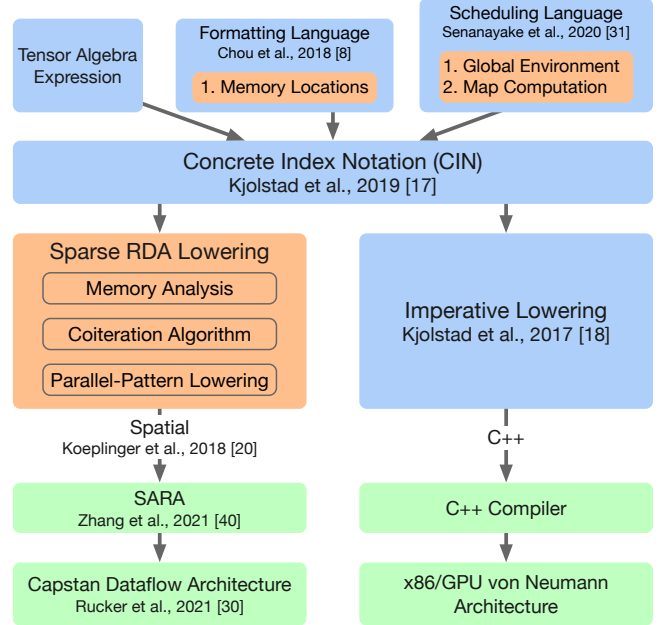


Figure 1. Overview of Stardust. Orange denotes new contributions, blue denotes prior work from the TACO literature, and green denotes the target compiler and hardware backends.

Figure 1 shows in orange the new format and scheduling language constructs we have added to Stardust that respectively map tensors and computation to the accelerator (Section 5). The memory location format construct lets the user denote that tensors live on the accelerator (Section 5.1), while the memory analysis algorithm in the lowering component automatically determines the exact accelerator memory (Section 6). And, the new map and accelerate commands let users map a sub-computation to the accelerator (Section 5.2), while the co-iteration algorithm automatically maps the pieces of the sub-computation to exact hardware implementations (Section 7).

3 Background

Our work builds on two lines of prior work, as shown in Figure 1. We add format and scheduling constructs to the set of constructs proposed by Chou et al. [8] and Senanayake et al. [31] and extend the concrete index notation of Kjolstad et al. [17]. By compiling to Spatial, we can reuse the SARA [40] compiler to Capstan.

3.1 Sparse Tensor Algebra Compilation

The TACO compiler separates the algorithm (tensor index notation) from the tensor compression formats and computation transformations through the use of format [8] and scheduling [31] languages, respectively. It compiles sparse tensor algebra to imperative code by decomposing sparse iteration spaces into hierarchical set expressions of per-dimension

Index Variable	i	Index Variable List	i^*	Constants	c	Tensors	\mathcal{T}
Accesses	a	$::= \mathcal{T}(i^*)$					
Expressions	e	$::= a \mid c \mid e + e \mid e * e \mid \dots$					
Statements	S	$::= \forall_i S \mid a = e \mid a += e \mid S ; S \mid S \text{ where } S \mid S \text{ s.t. } r^*$					
Scheduling Relation	r	$::= \text{split_up}(i, i_o, i_i, c) \mid \text{split_down}(i, i_o, i_i, c) \mid \text{fuse}(i_o, i_i, i_f) \mid \dots$					

Figure 2. Concrete index notation (CIN) syntax.

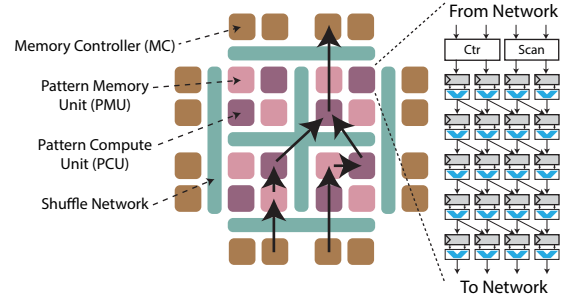
Scheduling Commands	Description
$\text{precompute}(e, i^*, i_w^*, \mathcal{T}) \rightarrow$ $\dots \forall_{i_o} a = e \xrightarrow{\text{precompute}(e, i^*, i_w^*, \mathcal{T})} \dots \forall_i a = \mathcal{T}(i^*) \text{ where}$ $\forall_{i_w^*} \mathcal{T}(i_w^*) = e[i_w^* / i^*]$	Inserts a where node to precompute a subexpression e into a temporary tensor workspace \mathcal{T} with new indices i_w^* on the right-hand side of the newly introduced where node.
$\text{split_up}(i, i_o, i_i, c) \rightarrow$ $\text{split_down}(i, i_o, i_i, c) \rightarrow$	Stripmines a forall into a nested outer i_o and constant-factor inner i_i foralls.
$\dots \forall_i S \xrightarrow{\text{split}^*(i, i_o, i_i, c)} \dots \forall_{i_o} \forall_{i_i} S \text{ s.t. } \text{split}^*(i, i_o, i_i, c)$	Stripmines a forall into a nested constant-factor outer i_o and inner i_i forall.
$\text{fuse}(i_o, i_i, i_f) \rightarrow$ $\dots \forall_{i_o} \forall_{i_i} S \xrightarrow{\text{fuse}(i_o, i_i, i_f)} \dots \forall_{i_f} S \text{ s.t. } \text{fuse}(i_o, i_i, i_f)$	Fuses two nested forall loops i_o, i_i into one i_f .
$\text{reorder}(i^*) \rightarrow$ $\dots \forall_i \forall_{j \dots} S \xrightarrow{\text{reorder}(j, i, \dots)} \dots \forall_j \forall_{i \dots} S$	Reorders the forall nodes based on a list of index variables i^* .

Table 1. Scheduling commands from TACO along with their CIN transformation [17, 18, 31]. $e[x'/x]$ denotes the expression e with each occurrence of x replaced by x' .

data structures. Sparse algorithms are expressed in CIN (see Figure 2), which encodes iteration, computation, transformations, and temporary tensors [17]. Finally, TACO lowers CIN to generate efficient fused code that traverses irregular data structures by skipping unnecessary computation.

Scheduling. The sparse scheduling language proposed by Senanayake et al. [31] provides a sparse iteration transformation framework. The framework modifies the sparse iteration space of an expression by taking its CIN statement and transforming it into a new CIN statement that represents a different algorithm for the same expression. The scheduling transformation framework describes optimizations to change the computation order, insert temporary tensors for partial sub-computation, exploit parallelism, and more. See Table 1 for a reference to the TACO scheduling commands.

Format Language. The format language proposed by Chou et al. [8] decomposes a sparse tensor into per-dimension (or level) formats that each describes how to store the coordinates of one dimension of a tensor. As an example, the canonical compressed sparse row (CSR) compression format


Figure 3. A high-level overview of the Capstan architecture, showing the opportunities for high-level parallelism across PCUs and vectorized parallelism within a PCU.

(see Figure 8 for an example matrix) can be represented by an uncompressed (dense) dimension followed by a compressed (sparse) dimension. After the tensors have been described using level formats and scheduling transformations have been applied to the CIN, TACO generates code that iterates over the level formats of the expression.

3.2 Capstan and Spatial

RDAs improve performance and efficiency by removing overhead found in CPUs and GPUs. RDAs map programs in space, meaning multiple data elements are processed in the same clock cycle by pipelined and parallel compute units.

Capstan [30], shown in Figure 3, is an RDA that targets sparse problems and is derived from Plasticine [27]. A notable Capstan architectural contribution is a *declarative-sparse model* for sparse iteration. This model divides sparse iterations into pattern headers and pattern bodies, where headers determine which (un)compressed iterations to run, and bodies use header iteration information to load, compute, and store data. An example of this paradigm for co-iteration of two compressed tensor levels can be found in Figure 7.

Capstan is programmed with Spatial [20],¹ a parallel-pattern hardware domain-specific language for FPGAs and RDAs. Spatial’s output is lowered to a streaming on-chip dataflow graph by the SARA compiler [40], which handles low-level optimizations and inserts memory-consistency logic.

Spatial uses a map-reduce abstraction. Each Foreach or Reduce pattern is counter-indexed with an explicit parallelization factor; multiple levels of nested loops can be independently parallelized to exploit different program-level parallelism opportunities. Typically, the innermost loop is vectorized, and the outermost loop is replicated across pattern compute units (PCUs). Capstan provides sparse iterator patterns—including union and intersection combinations—in addition to dense ones. Sparse patterns iterate by running on non-zero bit-vector elements using the index of the non-zero element instead of a counter. Sparse patterns are key to Capstan’s performance by enabling a declarative programming model (see Figure 9).

¹A full description of Spatial can be found at spatial-lang.org.

Spatial has an explicit, decoupled, programmer-managed memory hierarchy. In a CPU, memory is managed using caches and demand misses; however, Spatial requires manually partitioning data into chunks that fit on-chip and controlling the corresponding data movement. Specifically, there are four programmer-controlled memory types, ranging from far to near: DRAM, SRAM, FIFOs, and registers, with the middle two mapping to Capstan’s pattern memory units (PMUs).

4 Running Example

To illustrate the gap between compiling sparse expressions in imperative code versus code generation for RDAs, we will introduce a running example. Consider SDDMM (sampled dense-dense matrix multiplication), a sparse linear algebra kernel used in machine learning. SDDMM defined in index notation is $A(i, j) = B(i, j) * C(i, k) * D(k, j)$ where A and B are sparse (and in this case CSR) matrices. However, index notation does not specify low-level control flow. We can expand the index notation to the following imperative CIN:

$$\forall_i \forall_j \forall_k (A_{ij} += B_{ij} * C_{ik} * D_{kj}) \quad (1)$$

As shown in Figure 4a, there is a clear path from this CIN statement to an imperative programming model, and many compiler decisions in prior work presuppose this programming model: ❶ the \forall nodes are directly converted into for-loops, ❷ tensor accesses always load and store one element of the tensor at a time, ❸ tensor computation occurs only inside the innermost loop, and ❹ accumulations are implemented as temporally-repeated variable modifications.

To target a streaming spatial hardware backend, on the other hand, a compiler cannot leverage the above assumptions in the imperative programming model. Therefore, Stardust must address the following challenges when bridging the gap from an imperative to streaming spatial programming model: ❺ the \forall nodes must be traversed in a scanned fashion without temporal counters, ❻ data movement occurs between memory locations in vectorized streamed chunks parallelized across pipelines, ❼ tensor computation occurs when the data arrives as opposed to in the innermost loop, and ❽ parallel streams of computation are mapped in space to hardware resources. Figure 4b lays out the sparse SDDMM kernel as a streaming spatial program mapped onto the Capstan architecture, shown in Figure 3, illustrating the compilation gaps that Stardust needs to address. The compiler targets the Capstan hardware by reorganizing the computation into a spatial dataflow program using a declarative, parallel-pattern (map-reduce) based functional programming abstraction with explicit management of fixed-size memories [20].

5 Scheduling Computation for Accelerators

A sparse tensor algebra expression can be computed using many different algorithms on different data structures, which motivates the separation of expressions, schedules, and data representation (formats) [19, 28]. We introduce a new data representation property and scheduling language constructs. When combined with prior work on TACO formats [8, 18] and scheduling constructs [17, 31], they let end users reshape computation to expose sub-expressions that can be mapped to domain-specific accelerator patterns. Sparse domain-specific architectures (DSAs) are optimized for certain computation and iteration patterns dictated by the architectural decisions of the designer. Scheduling computation that efficiently (and correctly) maps to a hardware backend is key since these accelerator backends will have fixed resources, a fixed design, support for only certain features, and various tradeoffs. The scheduling transformation framework enables an end user, or an auto-scheduler, to exploit the hardware optimizations by reshaping the computation to expose sub-computation that will fit the target backend (with any other computation orchestrated by the host machine).

Stardust provides input languages that place tensors in explicit memory regions (to denote tensor scoping) and computation acceleration through specialized function mappings. We extend the data representation language of Chou et al. [8] with a new memory placement property that lets the user (or a future auto-scheduler) explicitly place tensor data structures in either *off-chip (global)* or *on-chip (local)* memory. Furthermore, we also extend the scheduling language framework presented by Senanayake et al. [31] with three new scheduling commands that map kernels to optimized, configured backend implementations. Finally, we demonstrate how a user can leverage the input languages to reshape computation to Capstan’s parallel patterns.²

Thus, we raise the abstraction of the low-level hardware to the high-level tensor input languages of Stardust and separate out the scheduling commands that map the computation to specialized hardware backends, which can be used by a hardware expert or by a future auto-scheduler.

5.1 Format Language: Explicit Tensor Memory Regions

The data representation API of Stardust lets a user place a tensor into their memory region of choice, which in our system is either off-chip memory or in the memory of the

²Although we target the Capstan parallel patterns in this work, the proposed scheduling construct can in future work be adapted to target other hardware accelerators or even hand-optimized library calls.

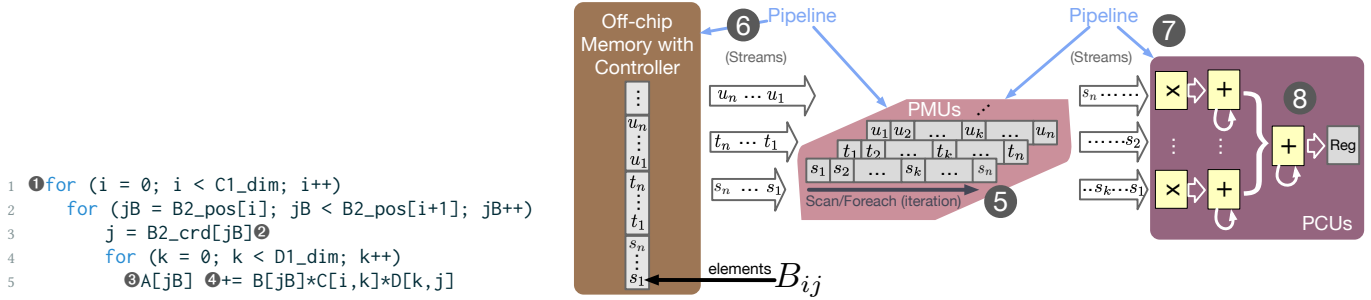


Figure 4. The SDDMM algorithm in an imperative programming model and as a spatial dataflow hardware configuration.

```

1 // Define off-chip (global) tensor formats
2 Format csr_off({uncompressed,compressed}, offChip);
3 Format rm_off({uncompressed,uncompressed}, offChip);
4 Format cm_off({uncompressed,uncompressed}, {1,0}, offChip);
5 // Declare input and output tensors
6 Tensor<int> A({N,N}, csr_off);
7 Tensor<int> B({N,N}, csr_off);
8 Tensor<int> C({N}, rm_off);
9 Tensor<int> D({N}, cm_off);
10
11 // Define SDDMM computation (algorithm).
12 IndexVar i, j, k;
13 A(i, j) = B(i, j) * C(i, k) * D(k, j);
14
15 // Scheduling language: Define environment variables
16 IndexStmt stmt = A.getAssignment();
17 stmt = stmt.environment(innerPar, 16);
18 stmt = stmt.environment(outerPar, 2);
19 // Precompute accumulation into a ws register
20 // to accelerate it using a Reduce pattern
21 Tensor<int> ws(on);
22 stmt = stmt.precompute(B(i,j)*C(i,k)*D(k,j), {}, {}, ws);
23 stmt = stmt.accelerate(forall(k, ws+=B(i,j)*C(i,k)*D(k,j)),
24                       Spatial, Reduction, innerPar);
25
26 // Perform computation by generating and executing code
27 std::cout << A << std::endl;
    
```

Figure 5. Abridged C++ Stardust input code for SDDMM.

accelerator.³ The off-chip memory region is globally accessible to all backends involved in the computation (host and accelerators) whereas on-chip tensors are only locally accessible locally to one backend. This memory region annotation within the format language is essential in denoting the scope in which specific tensor data lives (within a memory hierarchy), describing where tensor data should be initialized, and reasoning about what actions need to occur (like data transfers) to get the data in scope before computing on those tensor values.

³Users only state whether to place memory on the accelerator or not. Our accelerator, however, may have many different types of memories on-chip and our automated memory analysis determines which specific accelerator memory to use.

With the explicit memory region annotation, information to transfer input data to the accelerator (on-chip) or results back to the host (off-chip) is encoded within the CIN representation as an assignment statement. Moreover, the precompute scheduling command, together with the data representation API, lets users create new temporary tensors to store intermediate values and place them in accelerator memories. Our SDDMM example demonstrating the on- and off-chip communication API is shown in Figure 5 (with the final Spatial code generated by Stardust in Figure 11). Figure 6 then demonstrates the use of the precompute scheduling command to transfer data between different memory regions by inserting temporary tensor variables with a different memory region. We require the explicit on- versus off-chip placement (via the scheduling language) because input tensors could start out in various memory locations and host↔accelerator transfers could happen at multiple program locations. Figure 6 shows two schedules, along with their CIN, that use different memory regions. Separate on-chip and off-chip memory regions also let our compiler represent tensor partitioning (like blocking or tiling) on the host processor, with faster accelerated computation on-chip in the DSA.

5.2 Scheduling Language: Mapping Sub-computation

Through Stardust, users leverage schedules to reshape CIN sub-statements to expose sub-computations that can be mapped to high-level accelerated primitives, which in this paper are the Spatial parallel patterns. Given any CIN statement S that includes a sub-statement S' where $S \stackrel{\text{def}}{=} \dots S' \dots$, and S' has an equivalent instruction f for a given platform, the scheduling language can transform S such that S' is isolated. Then, the sub-statement S' can be replaced and computed using the specialized pattern or function f for a given backend instead of being lowered directly to code.

```

1 stmt = stmt.precompute(C(i,k), {k}, {k}, C_on)
2 stmt = stmt.precompute(D(k,j), {k}, {k}, D_on)
    $\forall_i \forall_j (\forall_k (A_{ij} += B_{ij} * C_k^{on} * D_k^{on})$ 
     where  $\forall_k (C_k^{on} = C_{ik})$ 
     where  $\forall_k (D_k^{on} = D_{kj})$ 

```

(a) New CIN after partial on-chip loads of C_{rows} and D_{cols} in the j -loop body using two precompute commands.

```

1 stmt = stmt.precompute(C(i,k), {i,k}, {i,k}, C_on)
2 stmt = stmt.precompute(D(k,j), {k,j}, {k,j}, D_on)
    $\forall_i \forall_j \forall_k (A_{ij} += B_{ij} * C_{ik}^{on} * D_{kj}^{on})$ 
     where  $\forall_i \forall_k (C_{ik}^{on} = C_{ik})$ 
     where  $\forall_j \forall_k (D_{kj}^{on} = D_{kj})$ 

```

(b) New CIN after initial load of C and D entirely before computation loops using two different precompute commands.

Figure 6. Two SDDMM schedules and their corresponding CIN statements demonstrating the mapping of formats on- and off-chip for accelerator backends (in contrast to the default schedule in eq. (1)). Tensors A, B, C^{on}, D^{on} have on-chip formats and C, D have off-chip formats.

Concretely, consider the simple vector-vector multiplication statement $S \stackrel{\text{def}}{=} S' \stackrel{\text{def}}{=} (\forall_i a_i = b_i * c_i)$ where all vectors are currently off-chip. Assuming there exists a vectorized multiplier block $f_{mul}(\text{out}, \text{in}_1, \text{in}_2)$ for a given backend, the `map` command can be used in conjunction with the `precompute` command to optimize the kernel. The transformation is demonstrated in equations 2–4:

$$S' \stackrel{\text{def}}{=} (\forall_i a_i = b_i * c_i) \xrightarrow{\text{precompute}(b_i * c_i, \{i\}, \{i\}, a^{on})} S'' \quad (2)$$

The above `precompute` transformation results in a new statement where the vector-vector multiplication result is stored into an on-chip result a^{on} and then the on-chip result is stored back off-chip into a .

Then, another `precompute` transformation is called for each off-chip input tensor so that the vector-vector multiplication is computed using only on-chip inputs

$$S'' \stackrel{\text{def}}{=} \left\{ \begin{array}{l} \forall_i a_i = a_i^{on} \xrightarrow{\forall t \in \{b, c\} \text{ precompute}(t_i, \{i\}, \{i\}, t^{on})} S''' \\ \text{where } \forall_i a_i^{on} = b_i * c_i \end{array} \right. \quad (3)$$

where t^{on} denotes an on-chip tensor format and t denotes an off-chip format for all $t \in \text{tensors}(e)$.

Lastly, the vector-vector multiplication kernel is mapped to the vectorized multiplier f_{mul} using only on-chip tensors as operands $f_{mul}(a^{on}, b^{on}, c^{on})$.

$$S''' \stackrel{\text{def}}{=} \left\{ \begin{array}{l} \forall_i a_i = a_i^{on} \xrightarrow{\text{map}(\forall_i a_i^{on} = b_i^{on} * c_i^{on}, \text{backend}, f_{mul})} \forall_i a_i = a_i^{on} \\ \text{where } \forall_i a_i^{on} = b_i^{on} * c_i^{on} \quad \text{where } f_{mul}(a^{on}, b^{on}, c^{on}) \\ \text{where } \forall_i b_i^{on} = b_i \quad \text{s.t. map}(\text{backend}, f_{mul}) \\ \text{where } \forall_i c_i^{on} = c_i \quad \text{where } \forall_i b_i^{on} = b_i \\ \quad \quad \quad \text{where } \forall_i c_i^{on} = c_i \end{array} \right. \quad (4)$$

We also introduce define a new `accelerate` scheduling command that combines all of these intermediate steps. This command is a compound command consisting of one or more `precompute` commands and a `map` command, and is necessary to map any sub-statement to a new backend function.

Given that $S \stackrel{\text{def}}{=} \dots S' \dots$ and $S' \stackrel{\text{def}}{=} \forall_{i*} a = e$, we define the `accelerate` transformation below.

$$S \xrightarrow{\text{accelerate}(S', \text{backend}, f, c)} S_{\text{new}} \quad (5)$$

is equivalent to

$$\dots S' \dots \xrightarrow{\text{precompute}(e, i^*, i^*, a^{on})} \xrightarrow{\text{For all } t \in \text{tensors}(e) \text{ precompute}(t_i, i^*, i^*, t^{on})} \xrightarrow{\text{map}(S' [t^{on}/t \text{ for all } t \in \text{tensors}(S')], \text{backend}, f, c)} S_{\text{new}} \quad (6)$$

Intuitively, the `accelerate` command first precomputes all off-chip tensors on-chip for a the sub-statement that is being accelerated and then maps the on-chip tensors to the backend function f for substituted computation.

We also describe a specific use-case for the `accelerate` command in our implementation targeting Spatial. This command is used to accelerate accumulations by calling Spatial’s `Reduce` pattern, which maps to Capstan’s optimized reduction tree hardware within a PCU. Stardust leverages the `accelerate` command to transform `forall-with-accumulation` patterns into a `Reduce` pattern (Figure 5, lines 28–30). More specifically, the `accelerate` command may be used with the `precompute` scheduling command to transform an accumulation loop $\forall(\dots += \dots)$ into a CIN sub-statement with the following `forall` pattern: $\forall(\dots = \text{ws where ws} += \dots)$, where ws is scalar. The transformed $\forall(\dots)$ statement is accelerated by replacing the CIN statement with a `Reduce` parallel pattern using the `accelerate` command (which under the hood calls the `map` command). Our compiler also has optimization passes that can automatically accelerate common CIN sub-statements to more optimized implementations. One such automatic scheduling pass detects CIN sub-statements that loop over an array transferring a single element of data at a time, $\forall(i, t_1(i) = t_2(i))$, and maps them to bulk memory load or store functions.

Finally, metadata must be passed directly to the global scope in order to configure the backends that call their specialized functions f when using the `map` and `accelerate` commands. Therefore, we introduce an `environment` command to set these metadata configuration variables to values. Lines 44–45 in Figure 5 shows the configuration of both the inner and outer parallelization factors to pass to the Spatial compiler [20]. With the `environment` command, users can use our compiler to search the design space of kernels parameterized by these metadata values. Specifically, an end-programmer can now perform design-space exploration of the backend hardware schedules and tensor-algebra kernels

Scheduling Commands	Description
$\text{map}(S, \text{backend}, f, c)$ $\dots S \xrightarrow{\text{map}(S, \text{backend}, f, c)} \dots f(\text{tensors}(S), V^\dagger, c)$ s.t. $\text{map}(\text{backend}, f)$	→ Maps a CIN statement S to a backend-specific computation strategy (specialized block, function, pattern, or instruction) f with some optional constant factor, c . Where V is the set of variables $\{i^*, r^*, \text{var}^*\}$ defined by the scope of the CIN sub-tree right before the statement S .
$\text{accelerate}(S, \text{backend}, f, c)$	→ A compound scheduling command that accelerates a sub-statement S by precomputing all tensors of S into on-chip tensors for a new expression S' and then maps an equivalent f onto S' (the new statement with all on-chip tensors). See eq. (5) for the formal transformation definition.
$\text{environment}(\text{var}, c)$ $S \xrightarrow{\text{environment}(\text{var}, c)} S$ s.t. $\text{var} = c$	→ Sets a global hardware configuration variable to some value, c .

Table 2. New scheduling commands necessary to target DSAs.

using high-level index notation and scheduling transformations (including global configuration parameters) without direct knowledge of the backend architecture or its programming model.

Although transformations of our SDDMM example in Figure 5 are very specific to parallel patterns, it demonstrates the importance of the input languages of Stardust in order to generate valid algorithms for any backend or pattern. The transformation framework can more generally be applied to any CIN statement and backend combination. A full list of scheduling commands needed to target the hardware from Stardust, and their corresponding descriptions, can be found in Table 1 and Table 2.

6 Memory Analysis

When compiling to accelerators, the compiler will often need to generate code to manage explicit fixed-length memories. Hardware accelerators (including GPUs) typically have memory hierarchies with multiple physical memory types that are explicitly managed by software, also called explicit, decoupled data orchestration [9, 14, 23, 26, 27, 30]. These memory types often have different capacities, transfer speeds, access patterns, and scopes (notably, only some are host-visible); the compiler must bind data structures to memories and generate transfers between them. The different sub-arrays involved in sparse tensors—coordinates, positions, and values—are also often mapped separately based on a combination of the sub-array and memory properties, complicating the analysis.

Stardust analyzes the memory needs of format-annotated CIN to generate Spatial kernels for Capstan. The format abstraction gives end users explicit control over tensor placement for one level of memory hierarchy, which we call *coarse-grained* memory pinning.

The compiler then automatically binds tensor format sub-arrays (positions, values, etc.) to Spatial memory types (which later become physical Capstan memory) using *fine-grained* memory pinning. The automatic inference analysis is crucial in avoiding unwieldy end-user memory management, which would require decisions on the Cartesian combination of: the number of input tensors for a kernel, levels per tensor, sub-arrays per level format, and the memory analysis for each sub-array (which includes memory type matching, memory allocation, and multiple data transfer locations). Finally, CIN assignment nodes are lowered to inter-region data transfers (e.g., DRAM to SRAM loads and vice versa). This analysis ensures that memory properties and preconditions are satisfied, ensuring valid placement of tensor arrays.

6.1 Fine-Grained Array Memory Inference

Stardust emits tensor sub-array allocations and memory transfers during top-down CIN traversal, accounting for memory access patterns and physical properties. Fine-grained memory binding addresses multiple issues: 1) which physical memory type to allocate for a given tensor array, 2) where (in which pattern body) to allocate the chosen physical memory, and 3) where (in which pattern body) should our compiler emit inter-memory transfers. Incorrect analysis—incompatible memory allocations, late allocations, and missed data transfers—will cause hardware simulation errors or invalid kernel computations. The memory binding analysis does not consider array sizes since it allocates the maximal possible size for one unit of memory; it assumes every array will fit in this size constraint based on computation tiling to the accelerator as described by the scheduling language.

Stardust ensures the following preconditions when binding format sub-arrays of tensors to physical memory types: **Dense DRAMs.** Arrays of every off-chip tensor (input and output) are placed in dense DRAM initialized by the host. **Sparse DRAMs.** These provide an interface for direct off-chip random accesses of sparse data. This is useful when there is no identifiable working set to bring on-chip.

Dense SRAMs. The system will only bind arrays with affine access patterns to dense SRAMs, including position arrays (addressed in an $addr, addr + 1$ fashion) and values arrays of fully dense formats (generally traversed linearly).

Sparse SRAMs. The system binds any on-chip, small, fixed-size arrays that have an access pattern with reuse but random accesses to sparse SRAMs.

Bit Vectors. Bit vectors are special on-chip integer streams (Figure 7) that hold compressed coordinate information. Stardust automatically generates and manages bit vectors whenever a compressed-compressed co-iteration occurs.

FIFO Buffers. Arrays accessed linearly with certain access patterns may be bound to (seemingly infinite) FIFO buffers. The compiler cannot enqueue excess data that is not popped, cannot pop data before its storage lifetime ends, and must pop the data precisely when the storage lifetime ends. This

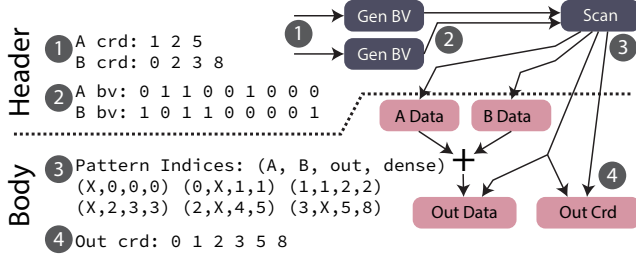


Figure 7. Element-wise co-iteration of two compressed vectors in Capstan. A sparse bit-vector scanner divides the problem into parallel map iterations, followed by memory atomics and reductions (pink blocks denote physical memories).

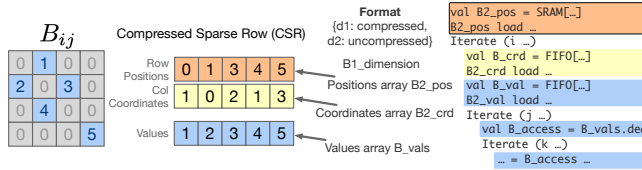


Figure 8. Example sparse B matrix used in SDDMM with its corresponding data structure and format arrays. The right details Spatial pseudocode generated by our work, demonstrating array memory allocations, accesses, and data transfers interleaved into the computation.

restricts FIFOs to coordinate arrays of sparse tensors and value arrays that are accessed in order.

Registers. On-chip scalar variables are bound to registers.

6.2 Data Transfer Analysis

After the compiler has chosen an accelerator memory type for a tensor, it inserts code to allocate memory and to transfer data to and from the memory. Tensor arrays are allocated at the loop level just above their first use, for ease of analysis, but hoisting them and inserting reset code between iterations is also possible.

Sparse tensors have multiple index arrays and a value array whose data must be transferred to and/or from the accelerator. Their value arrays store the actual values, while each of its compressed level stores the compressed indices in two arrays: positions and coordinates. Consider our running SDDMM example (illustrated in Figure 8), where B 's CSR format list (an uncompressed/dense dimension followed by a compressed dimension) describes the access B_{ij} , as well as the iteration over the index variables $\{i, j\}$ and the loops $\forall_i \forall_j$. The innermost level of B corresponds to the index variable j and iterates over the position and coordinate arrays $B2_pos$ and $B2_crd$, respectively. This means both B_vals and $B2_crd$ elements will be accessed inside the j -loop, so both arrays must be allocated right before in the i -loop body, with $B2_pos$ being accessed in the i -loop and allocated at the top.

Our lowering algorithm ensures tensors are filled with values before their use by making the following assumptions:

```

1 // Uncompressed iteration and reduction
2 Foreach(len by inc par p) {i_dense => ...}
3 Reduce(reg)(len by inc par p) {i_dense => ...}
4 MemReduce(mem par mp)(len by inc par p) {i_dense => ...}
5 // Compressed single iteration (Reduce not shown)
6 Foreach(len by inc par p) {pos => ...}
7 Foreach(Scan(par=p, len=1, bitvector_A.deq))
8   {A, i_dense => ...}
9 // Compressed-compressed coiteration (Reduce not shown)
10 Foreach(Scan(par=p, len=1, bitvector_A.deq,
11   bitvector_b.deq)) {A, B, out, i_dense => ...}

```

Figure 9. Spatial parallel patterns for compressed (sparse) and uncompressed (dense) mode-level iterations.

1) value-array elements are always accessed at the corresponding loop body of the innermost mode of a tensor, 2) coordinate array elements are always accessed at the index loop body corresponding to that mode, and 3) position array elements are always accessed one loop higher. If a higher loop does not exist, the arrays are accessed at the start of the kernel. All allocations occur before the loop header of the current loop (also the loop body of the preceding loop-*nest*), and all data transfers occur immediately after their associated allocations.

Our lowering algorithm must access value elements at the loop body of a tensor's innermost mode and not lower in the loop-*nest* hierarchy. We may not assume that array elements are accessible anywhere after array declaration because this is not possible for memories that do not support random access. Using a FIFO for an in-order traversal of the modes, for example, requires that the FIFO values be accessed precisely at the level of the last tensor mode and only used for one iteration of that loop. Figure 8 demonstrates that if the value array of B_{ij} was bound to a FIFO with the iteration pattern of the computation as $\forall_i \forall_j \forall_k$, the B_vals array elements would have to be accessed in the j -loop (corresponding to B 's last mode) instead of the k -loop (the innermost loop) as in the CPU case.

With our memory analysis, we simplify end-user programming. Users decide only whether the tensor is on-chip or off-chip, while our compiler manages the fine-grained arrays associated with each compressed tensors. Our algorithm design also lets Stardust perform lowering transformations and optimizations at a fine-grained (per-array) level.

7 Co-iteration Lowering as Rewrite Rules

In many situations, DSAs and accelerators accelerate computation using streams of data. These streams flow through functional hardware blocks that produce new output streams. Because the blocks are functional mappings from input to output streams, general-purpose control flow statements like conditionals are no longer available, TACO's lowering machinery can no longer be used.

7.1 Co-iteration Rewrite System

Sparse accelerators further speed up sparse tensor computations by contracting together tensor elements efficiently, and a good compiler must support these algorithms natively. For example, DSAs may have specialized hardware blocks with clever algorithms and optimized data structures to increase performance, such as the examples in Figure 9. One such data structure is the bit-vector format, which densely packs sparse coordinate information [7, 30]. The bit-vector format accelerates kernels by enabling hierarchical intersections using bit-vector trees, uncompressed blocked iteration of sparse data, and efficient tensor contractions using boolean logic.

Stardust introduces a rewrite system for matching fused iteration patterns to a corresponding backend behavior, which is shown in Figure 10. The lowering mechanism traverses the CIN IR recursively. When a CIN forall node is found, the lowerer decomposes the level’s fused tensor iterator contraction set, $I = \mathcal{T}_1 \circ \mathcal{T}_2 \circ \dots \circ \mathcal{T}_n$ s.t. $\circ \in \{\cup, \cap\}$, $n \geq 1$, into smaller tensor iterator contraction subsets based on the iterator formats for that level and the contraction type. The tensor iterator contraction subsets generated are those supported by the backend. For example, if a backend has a custom instruction, or-and, to compute $(a \cup b) \cap c$ given three compressed inputs, its rewrite rule would be: $\text{lowerIter}[(C_1 \cup C_2) \cap C_3] \Rightarrow \text{emit or-and}$. If a backend does not have a rewrite rules (e.g., intersection but not union support), the rewriter will map unmatched computations to the host.

7.2 Scheduled CIN Lowering Implementation

Lowering from a scheduled CIN statement to Spatial parallel patterns is straightforward. Environment variables set by the schedule are emitted first so that they are globally scoped. Next, Stardust recursively traverses the CIN and replaces map-scheduled statements with optimized hardware functions or instructions. To demonstrate, the example on line 34 in Figure 5 would cause the lowerer to emit a Reduce pattern. Stardust then automatically lowers remaining \forall nodes (those not scheduled with a map) to the *declarative-sparse programming model* (see fig. 10). Instead of mutable counters, the compiler determines the iteration space (min until max by step) and uses pattern indices within the body to access tensor data.

When needed, elements of one to two input tensor coordinate arrays are streamed into a packed bit vector, as shown in Figure 7. The packed bit vector stores compressed coordinate information using a 1 where a coordinate is nonzero and a 0 at all other positions. Two compressed bit vectors are then either logically AND-ed (for intersection/multiplication) or OR-ed (for union/addition) by the sparse bit-vector scanner, depending on the tensor algebra operator. The system then emits two scanner loops: one calculates position sub-array

Let the set of iterator contractions for a given \forall node be:

$$I = \mathcal{T}_1 \circ \mathcal{T}_2 \circ \dots \circ \mathcal{T}_n \text{ s.t. } \circ \in \{\cup, \cap\}, n \geq 1$$

Let $\text{format}(I) = \text{format}(\mathcal{T}_1) \circ \text{format}(\mathcal{T}_2) \circ \dots \circ \text{format}(\mathcal{T}_n)$
 $\text{format}(\mathcal{T}_n) = C_n$ if \mathcal{T}_n is compressed, $\text{format}(\mathcal{T}_n) = \mathcal{B}_n$ if \mathcal{T}_n is a bit vector, $\text{format}(\mathcal{T}_n) = \mathbb{U}$ (the universe) otherwise.

	$\text{lowerIter}[\text{format}(I)] \Rightarrow \text{emit } \langle \text{backend block behavior} \rangle$
Single-Iteration	$\text{lowerIter}[\mathbb{U}] \Rightarrow \text{emit } \langle \text{Foreach or Reduce}(\dots \Rightarrow i \dots) \rangle$
	$\text{lowerIter}[\mathcal{B}_1] \Rightarrow \text{emit scanner for result positions}$ $\text{emit } \langle \text{Foreach}(\dots \Rightarrow \text{pos} \dots) \rangle$
	$\text{lowerIter}[C_1 \text{ and } \mathcal{T}_1 \text{ is result}] \Rightarrow \text{emit } \mathcal{B}_1 = \text{GENBITVECTOR}(\mathcal{T}_1)$ $\text{lowerIter}(\mathcal{B}_1)$
	$\text{lowerIter}[C_1] \Rightarrow \text{emit } \langle \text{Foreach}(\dots \Rightarrow \text{pos} \dots) \rangle$
Universe	$\text{lowerIter}[\mathbb{U} \cup _] \Rightarrow \text{lowerIter}(\mathbb{U})$
	$\text{lowerIter}[_ \cup \mathbb{U}] \Rightarrow \text{lowerIter}(\mathbb{U})$
	$\text{lowerIter}[\mathbb{U} \cap \mathbb{U}] \Rightarrow \text{lowerIter}(\mathbb{U})$
Comp.	$\text{lowerIter}[C_1 \cap \mathbb{U}] \Rightarrow \text{lowerIter}(C_1)$
	$\text{lowerIter}[\mathbb{U} \cap C_2] \Rightarrow \text{lowerIter}(C_2)$
Co-Iteration	$\text{lowerIter}[C_1 \circ C_2] \Rightarrow \text{emit } \mathcal{B}_1 = \text{GENBITVECTOR}(\mathcal{T}_1)$ $\text{emit } \mathcal{B}_2 = \text{GENBITVECTOR}(\mathcal{T}_2)$ $\text{lowerIter}(\mathcal{B}_1 \circ \mathcal{B}_2)$
	$\text{lowerIter}[\mathcal{B}_1 \circ \mathcal{B}_2] \Rightarrow \text{emit scanner for result positions}$ $\circ = \cup \Rightarrow \text{emit } \langle \text{Foreach}(\text{Scan}(\dots \text{or} \dots \Rightarrow i \dots)) \rangle$ $\circ = \cap \Rightarrow \text{emit } \langle \text{Foreach}(\text{Scan}(\dots \text{and} \dots \Rightarrow i \dots)) \rangle$
Base	$\text{lowerIter}[_] \Rightarrow \text{format}(\mathcal{T}_{1k}) = \text{lowerIter}(\mathcal{T}_1 \circ \dots \circ \mathcal{T}_k)$, largest $k \leq n$ that produces a match $\text{lowerIter}(\text{format}(\mathcal{T}_{1k} \circ \dots \circ \mathcal{T}_n))$

Figure 10. General rewrite system that lowers combined tensor iteration and contractions to declarative constructs (found in Figure 9), called by the LOWER function which recursively traverses the CIN IR and emits low-level IR. Specifically, this algorithm lowers \forall nodes to the declarative-sparse programming model of sparse iteration theory. Blue statements have side effects that emit low-level IR code.

entries by counting the number of nonzero results, and the other computes entries for the value sub-array.

Finally, LOWER recurses on the computation in the body of the second scanner, using atomic accesses to sparse SRAMs for future value-array computation. This lowerer implementation eliminates the need for temporal loads/stores, conditional control flow (if-statements and while-loops), and tensor union decomposition (into unions of disjoint intersections). Figure 11 shows the final Spatial code outputted by Stardust for our SDDMM running example.

8 Evaluation

We demonstrate significant performance improvements when using Stardust to target an RDA over compiling to a CPU or GPU, showing the usefulness of our compiler from the perspective of a data analyst or computational end user interested in a fast sparse tensor algebra library. And from the perspective of a performance/hardware engineer tasked with utilizing a sparse accelerator, our results show that Stardust provides increased productivity compared to writing

```

1 // Spatial header code
2 ...
3
4 // Initialize all DRAM arrays
5 val A2_pos_dram = DRAM[T](nnz_max)
6 ...
7
8 Accel {
9   val B2_pos = SRAM[T](nnz_accel_max)
10  B2_pos load B2_pos_dram(0::(B1_dim + 1) par ip)
11  Foreach (C1_dim by 1 par bp) { i =>
12    val A_vals = FIFO[T](16)
13    val A2_crd = FIFO[T](16)
14    val A2_pos = SRAM[T](nnz_accel_max)
15
16    val jB_start = B2_pos(i)
17    val jB_end = B2_pos((i + 1))
18    val jB_len = jB_end - jB_start
19
20    val B2_crd = FIFO[T](16)
21    B2_crd load B2_crd_dram(jB_start::jB_end par 1)
22    val B_vals = FIFO[T](16)
23    B_vals load B_vals_dram(jB_start::jB_end par 1)
24
25    Foreach (jB_len by 1 par 1) { jB =>
26      val j = B2_crd.deq
27      val B_hoisted = B_vals.deq
28
29      val D_vals = SRAM[T]((nnz_accel_max / 4))
30      D_vals load D_vals_dram((j*D1_dim)::((j+1)*D1_dim) par ip)
31      val C_vals = SRAM[T]((nnz_accel_max / 4))
32      C_vals load C_vals_dram((i*C2_dim)::((i+1)*C2_dim) par ip)
33
34      val tjA_vals = Reg[T](0.to[T])
35      Reduce(tjA_vals)(D1_dim by 1 par ip) { k =>
36        ((B_hoisted * C_vals(k)) * D_vals(k))
37      } { _ + _ }
38      A_vals.enq(tjA_vals)
39      A2_crd.enq(j)
40    }
41    A2_pos(i + 1) = jB_end
42    A_vals_dram stream_store_vec(jB_start, A_vals, jB_len)
43  }
44 }

```

Figure 11. SDDMM Spatial code generated by Stardust.

Name	Expression	Lines of Code	
		Input	Spatial
SpMV	$y_i = \sum_j A_{ij}x_j$	10	44
Plus3	$A_{ij} = B_{ij} + C_{ij} + D_{ij}$	8	91
SDDMM	$A_{ij} = \sum_k B_{ik}C_{kj}D_{jk}$	17	62
MatTransMul	$y_i = \sum_j \alpha A_{ji}^T x_j + \beta z_i$	13	50
Residual	$y_i = b_i - \sum_j A_{ij}x_j$	9	48
TTV	$A_{ij} = \sum_k B_{ijk}c_k$	13	73
TTM	$A_{ijk} = \sum_l B_{ijl}C_{kl}$	11	83
MTTKRP	$A_{ij} = \sum_{kl} B_{ikl}C_{jk}D_{jl}$	15	86
InnerProd	$\alpha = \sum_{ijk} B_{ijk}C_{ijk}$	11	115
Plus2	$A_{ijk} = B_{ijk} + C_{ijk}$	6	163

Table 3. The expressions used to evaluate our compiler.

the applications in a low-level language at the abstraction of the hardware.

8.1 Methodology

We evaluate Stardust using the same sparse tensor algebra expressions as in the original tensor compiler (TACO) paper [18], which can be found in Table 3. To improve on-chip parallelism, we map Plus3 as an iterated two-input addition because mapping Plus3 natively would only use half of Capstan at a time (performing the first addition and then the

App	Name	Dimensions	Density
SpMV SDDMM MatTransMul Residual	bsstk30 [10]	28924×28924	2.48×10^{-3}
	ckt11752_dc_1 [10]	49702×49702	1.35×10^{-4}
	Trefethen_20000 [10]	20000×20000	1.39×10^{-3}
Plus3	random	800×800	1.00×10^{-2}
	random	800×800	10.00×10^{-2}
	random	800×800	50.00×10^{-2}
TTV, TTM MTTKRP InnerProd Plus2	facebook [36]	$1591 \times 63891 \times 63890$	1.14×10^{-7}
	random	$200 \times 200 \times 200$	1.00×10^{-2}
	random	$200 \times 200 \times 200$	10.00×10^{-2}
	random	$200 \times 200 \times 200$	50.00×10^{-2}

Table 4. The datasets we use for evaluation.

	Par	PCU		PMU		MC		Shuf	
		#	%	#	%	#	%	#	%
SpMV	16	44 (22%)		41 (21%)		35 (44%)		16 (100%)	
Plus3	8	55 (28%)		100 (50%)		58 (73%)		8 (50%)	
SDDMM	12	163 (82%)		90 (45%)		61 (76%)		0 (0%)	
MatTransMul	16	47 (24%)		66 (33%)		36 (45%)		16 (100%)	
Residual	16	43 (22%)		65 (33%)		36 (45%)		16 (100%)	
TTV	16	93 (47%)		91 (46%)		67 (84%)		16 (100%)	
TTM	12	161 (81%)		89 (45%)		70 (88%)		0 (0%)	
MTTKRP	8	140 (70%)		70 (35%)		58 (73%)		0 (0%)	
InnerProd	8	53 (27%)		155 (78%)		80 (100%)		0 (0%)	
Plus2	1	10 (5%)		23 (12%)		14 (18%)		2 (13%)	

Table 5. Capstan resources required by our compiled kernels. The specific limiting resource(s) are shown in bold type.

second). CPU baselines are profiled using 128 threads on a four-socket Xeon E7-8890 v3 with a 32 KiB L1 data cache, 32 KiB L1 instruction cache, 256 KiB L2 cache, 46 080 KiB L3 cache, and 1024 GiB RAM. The machine runs Ubuntu 18.04.3 LTS and is clocked at 2494 MHz. We compile TACO using GCC 7.4.0 with OpenMP enabled. GPU baselines are profiled on an AWS EC2 p3.2xlarge instance with an NVIDIA V100 SXM-2 GPU. The GPU contains 64 KiB registers and 12 KiB L0 instruction cache per block, 128 KiB L1 data cache and shared memory and 2 KiB L1 constant cache per streaming multiprocessor (SM), and 6144 KiB L2 cache per GPU. The device RAM is 16 160 MiB. The GPU has 84 Volta SMs and is clocked at up to 1328 MHz. Kernels generated by TACO are compiled with NVCC version 10.0.0. When timing the kernels, we exclude data transfer time between the host and the GPU. Both baselines are run with a cold cache and using a single iteration.

Capstan applications are evaluated with the same cycle-accurate simulator originally used to evaluate Capstan [30]. The simulator uses an accurate model of the on-chip network, which accounts for delay and throughput constraints [38]; it also uses Ramulator [16] to model either four channels of DDR4-2133 or HBM-2E (at 1800 GB/s). The ideal network and memories are more performant since they do not consider latency and any slowdowns, HBM-2E has the highest real-technology memory bandwidth, and DDR4 is slowest.

All evaluations use the datasets shown in Table 4. For most 2-D kernels, we use the kernels demonstrated in the

Platform (Memory)	Compiled	Matrix Kernels					Tensor Kernels					gmean	
		SpMV	Plus3	SDDMM	MatTransMul	Residual	TTV	TTM	MTTKRP	InnerProd	Plus2		
Capstan (HBM2E)	No	0.65	—	—	—	—	—	—	—	—	—	—	0.65
Capstan (Ideal Net & Mem)	Yes	0.77	0.24	0.78	—	0.75	0.75	0.49	0.57	0.44	0.35	0.42	0.52
Capstan (HBM2E)	Yes	1.00	1.00	1.00	—	1.00	1.00	1.00	1.00	1.00	1.00	1.00	1.00
Capstan (DDR4)	Yes	12.13	10.07	8.33	—	12.31	12.06	4.92	9.80	7.76	3.28	1.72	7.09
Plasticine (HBM2E)	No	8.72	—	—	—	—	—	—	—	—	—	—	8.72
V100 GPU	Yes	3.15	41.89	18,259.50	—	3.59	3.54	232.85	284.47	6.77	2.76	381.38	41.31
128-Thread CPU	Yes	27.90	236.40	220.28	—	376.52	384.08	335.99	8.47	398.72	178.34	59.22	138.07

Table 6. Runtimes (geomean across all datasets) normalized to the compiled HBM-2E version of each application for different backends and memories. We compile to Capstan while TACO compiles to CPUs and GPUs. Only SpMV has handwritten kernels.

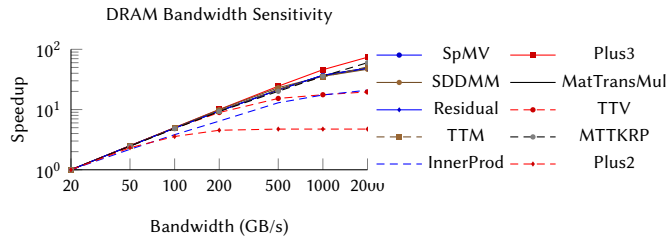


Figure 12. Impact of memory bandwidth on performance.

original Capstan paper [30]. However, Capstan’s bit-vector format does not natively support performant co-iteration on highly sparse (less than about 5%) tensors. Therefore, we use random datasets with higher densities for these applications (Plus3, InnerProd, and Plus2); these datasets are designed to match Capstan’s assumptions about data distribution. With different backends [9, 14], the ideal sparsity ratio would change.

For Plus3, we generate two additional datasets by rotating the input matrix’s columns right by one and two. For Plus2 and InnerProd, we generate one additional dataset by rotating the even coordinates on the last tensor dimension by one. Other than the SDDMM and MTTKRP matrices C and D (which are dense), we use CSR (or compressed sparse column (CSC) for MatTransMul) formats for all 2-D matrices. We use compressed sparse fiber (CSF) for most 3-D tensors and a CSR-like uncompressed-compressed-compressed format for InnerProd and Plus2.

The above formats are used for all platforms except for the GPU baseline which has different result tensor formats. Input tensor formats for GPU baseline are the same as above, but output tensors are fully dense. This is because TACO currently does not support sparse output tensors for their GPU backend.

8.2 Resource Consumption

For reference, Capstan is built as a grid of 200 vectorized compute units (PCUs) and 200 memory units (PMUs) that are ringed by 80 memory controllers (MCs), as shown in Figure 3. Each PCU has six stages and 16 vector lanes that can perform fixed or floating-point operations. Each PMU has 16 banks of 4096 32-bit words, supporting one read and

one write per bank every cycle. Capstan natively supports sparsity within its architecture by including sparse on-chip memory scheduling, fixed- and floating-point atomics, and sparse iteration over compressed bit-vector data structures. Additionally, 16 shuffle networks enable sparse accesses beyond the 16 lanes of a single PMU, but when used they limit the total number of outer-parallel iterations to 16.

To make good use of Capstan’s hardware, a compiler must be able to extract parallelism at both an inner-loop (vectorization) and outer-loop (cross-PCU) level. Outer-loop parallelism is harder to extract because it requires the compiler to explicitly distribute memories, including FIFOs which must be precisely enqueued and dequeued, across physically unrolled partitions. Based on the nature of Capstan’s distributed compute and memory resources, it is unlikely that an application could use 100% of all on-chip resources. Limiting resources vary, but all applications except Plus2 make good use of resources via outer parallelization because they approach a limit in at least one dimension (compute, memory, or shuffle-network ports). By hitting physical resource limits, the compiler ensures that users are able to take full advantage of Capstan.

One of the key factors in RDA (and GPU) out-performance is a high-bandwidth memory system. Capstan has support for either HBM-2E and DDR4 random access memory. Figure 12 shows that our applications (excepting Plus2, which is not outer-parallelized) are able to make good use of DRAM bandwidth as well. This is a direct result of the decoupled access-execute memory model: factoring out off-chip memory accesses into large, bulk loads and stores exposes significant memory parallelism.

8.3 Case Study: Sparse Matrix-Vector Multiplication

Sparse matrix-vector multiplication (SpMV) is the simplest of our applications and the only one where a handwritten Spatial implementation exists, as it is significant work to hand-implement a sparse tensor algebra kernel. A comparison of SpMV across all platforms is in the first column of Table 6. The Capstan and Plasticine rows from Table 6 are handwritten Spatial SpMV kernels from [27, 30] respectively.

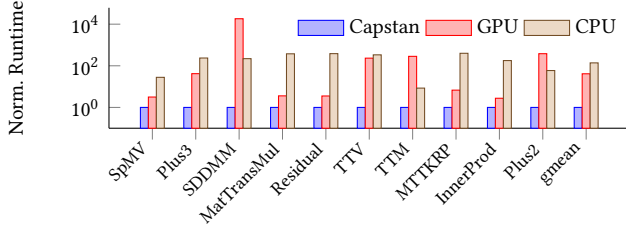


Figure 13. Generated kernel performance across three platforms normalized to Capstan. Our system is used to compile to Capstan and TACO is used to compile to the CPU and GPU.

All Capstan and Plasticine rows in Table 6 that are not compiled (where the Compiled column is No) are hand-written Spatial SpMV kernels. All of our SpMV evaluations use CSR matrices.

SpMV is simpler, making it is easy to parallelize; therefore, SpMV applications compiled by Stardust have a speedup relative to the CPU and GPU that is lower than other applications. However, the version of SpMV run in the original Capstan paper (Capstan, uncompiled) is more optimized than the compiled version (Capstan, compiled) because the code generated by Stardust uses the shuffle network (shown by SpMV×Shuf in Table 5) to coordinate parallel accesses to the input vector and the hand-written Capstan SpMV does not. Instead, the hand-written Capstan SpMV duplicates the input vector, which avoids shuffle-network contention and permits outer-parallelization beyond the shuffle network’s limit of 16. We expect that these additional optimizations can be automated in the future, but for now they demonstrate that a dedicated hardware expert can get better performance compared to Stardust, albeit at the cost of significant development effort.

To demonstrate that Stardust both increases programmer productivity and decreases development effort in targeting Capstan, we compare the lines of code (LOC) of the hand-written Spatial SpMV kernel against the Stardust kernel for Capstan. The compiled SpMV kernel uses 10 input LOC total—a 76% decrease from the 52 lines of Spatial required for the hand-written version. Moreover, we believe that the input code to Stardust is simpler to write and to port to new architectures. The code required for Stardust includes: 3 LOC for the tensor formats, 2 LOC for the algorithm, 4 LOC for the scheduling transformations, and 1 LOC to compile and output our kernel. With the use of an auto-scheduler, the number could be cut down from 10 to 6 LOC due to the removal of the user-provided schedule. These numbers support the use of our compiler as a programmer productivity tool for creating arbitrary sparse tensor kernels on accelerators.

8.4 Tensor Algebra Expression Performance

Performance results for all platforms and applications are shown in Table 6, with a subset of results for only Stardust

compiled Capstan, the TACO compiled GPU, and the TACO compiled CPU shown in Figure 13. The applications compiled by Stardust are, on average, 138× faster than CPU baselines, and 41× faster than GPU variants. These performance benefits motivate using RDAs—and thus a compiler to target RDAs.

Our TACO GPU baseline performance is significantly worse than both the literature [31] and compiled Capstan because TACO does not natively support sparse tensor outputs. Most of the time is spent zero initializing the fully dense result tensor—which is often extremely large—in device memory. Because Capstan is designed to outperform the GPU for sparse applications, it may seem counter-intuitive that the GPU speedup for MTTKRP is relatively low. However, these kernels have a dense dimension that the GPU can vectorize.

A comparison of compiled Spatial applications to hand-written Spatial implementations for Capstan across the applications is not possible, since handwritten kernels do not exist, except for SpMV. They do not exist because each application must be written by a Spatial, Capstan, and application/sparsity domain expert. Additionally, a handwritten implementation is slower to write since the Spatial programming abstraction is at a lower-level. In order to hand-write correct Spatial for Capstan, the domain expert must have deep knowledge of the Spatial-to-Capstan compilation process through both the Spatial and SARA compilers. The fact that our system is able to compile to applications where a hand-written Spatial implementation does not exist motivates the use of our automated compiler to generate the long tail of sparse tensor algebra kernels, which have practical applications, including deep neural networks (SDDMM), scientific computing (Plus3), linear least squares (Residual), and alternating least squares (MTTKRP).

9 Related Work

Stardust is, to the best of our knowledge, the first compiler to compile a high-level sparse tensor algebra expression language to a general sparse domain-specific accelerator. There is, however, prior work on sparse tensor algebra systems targeting CPUs and GPUs, compilers for dense image processing and neural network applications that target dense domain-specific architectures, other sparse domain-specific hardware that provides alternative targets for a compiler like ours, and different methodologies for programming these sparse DSAs.

Sparse Tensor Algebra Systems and Compilers. Several compilers have been proposed for sparse tensor algebra, but these compilers target CPUs [6, 15, 18, 21, 35] or GPUs [31], whereas our system compiles to domain-specific sparse dataflow hardware. We chose to extend TACO with a

compilation path to target RDAs since it contains input languages and IRs that support general tensor compression formats, optimizations, and expressions. TACO, unlike our system, defines co-iteration as only the intersection of tensor coordinates. In order to support all tensor algebra expressions, TACO uses an iteration lattice IR to decompose all unions of coordinates into disjoint intersections and then emits code that performs a multi-way merge strategy, whereas Stardust emits scanners through logical operations on bit vectors.

Sparse Domain-Specific Hardware. Other architectures have been proposed for single-function sparse acceleration, including matrix-vector multiplication [13] and matrix-matrix multiplication [25, 33, 37, 41]. Prior work has also mapped algorithms like SpMV [12, 32, 34, 39] to FPGAs. Because the compiler would not reconfigure the FPGA itself, pre-defined FPGA implementations would be exposed to the programmer in the same manner as an ASIC. From a compiler perspective, these algorithms can all be considered as special-purpose lowering cases. For example, a sparse matrix-matrix multiply could be mapped to our `accelerate` command.

Mapping Sparsity to DSAs. We focused our evaluation on Capstan [30] because it is a flexible RDA with an easy-to-understand programming model: it supports vectorized sparse iteration with composable parallel patterns. However, sparse iteration spaces are a general representation, and Stardust could target any reconfigurable sparse accelerator with appropriate backend modifications. The SPU [9] and ExTensor [14] are two recent sparse DSAs with different programming models than Capstan. Both have tiled architectures with explicit on-chip memory accesses, but they have different methods for combining sparse data.

The SPU uses a stream-join programming abstraction to combine sparse indices and a custom RDA fabric to perform the intersection operations. The core of stream-join is a conditional-dequeue abstraction with FIFO inputs: to lower to this abstraction, our compiler would have to rewrite CIN traversal using FIFO dequeues (instead of the pointer bumps and memory accesses used for CPU backends). Similarly, ExTensor uses a programming model based on hierarchical tensor intersector; these are designed to provide high throughput for direct iteration on sparse data structures. However, any compiler would still need to handle low-level mapping, including coordinating memory transfers.

10 Conclusion

We have described the first compiler that automatically compiles arbitrary sparse tensor algebra kernels to sparse reconfigurable dataflow accelerator. Since architects are developing many accelerators for sparse computations, we expect Stardust to be the first of many to target sparse accelerators. We expect its design—leveraging the separation of application code from both data representation *and* schedules to

independently map data to memories and (sparse) operations to sparse data combiners and compute units—will influence future domain-specific compiler designs. Finally, we plan to further extend our compiler path into a compiler toolkit that can be used to create sparse tensor algebra compiler backends for a host of emerging domain-specific sparse hardware.

11 Acknowledgements

We thank Willow Ahrens, Stephen Chou, Scott Kovach, Aviral Pandey, and Rohan Yadav for their helpful feedback and discussion. Olivia Hsu was supported by an NSF GRFP Fellowship, and Alexander Rucker was supported by a Stanford Graduate Fellowship. This work was supported in part by the NSF under grant numbers 1937301, 2028602, CCF-1563078, and 1563113. This research was also supported in part by the Google Research Scholar program, Facebook Systems for ML research award, and Stanford Data Analytics for What’s Next (DAWN) Affiliate Program. Any opinions, findings, and conclusions or recommendations expressed in this material are those of the authors and do not necessarily reflect the views of the aforementioned funding agencies.

References

- [1] Martín Abadi, Paul Barham, Jianmin Chen, Zhifeng Chen, Andy Davis, Jeffrey Dean, Matthieu Devin, Sanjay Ghemawat, Geoffrey Irving, Michael Isard, et al. 2016. Tensorflow: A system for large-scale machine learning. In *12th USENIX Symposium on Operating Systems Design and Implementation (OSDI 16)*. 265–283.
- [2] Andrew Adams, Karima Ma, Luke Anderson, Riyadh Baghdadi, Tzu-Mao Li, Michaël Gharbi, Benoit Steiner, Steven Johnson, Kayvon Fatahalian, Frédo Durand, and Jonathan Ragan-Kelley. 2019. Learning to Optimize Halide with Tree Search and Random Programs. *ACM Trans. Graph.* 38, 4, Article 121 (jul 2019), 12 pages. <https://doi.org/10.1145/3306346.3322967>
- [3] Luke Anderson, Andrew Adams, Karima Ma, Tzu-Mao Li, Tian Jin, and Jonathan Ragan-Kelley. 2021. Efficient Automatic Scheduling of Imaging and Vision Pipelines for the GPU. *Proc. ACM Program. Lang.* 5, OOPSLA, Article 109 (oct 2021), 28 pages. <https://doi.org/10.1145/3485486>
- [4] Krste Asanovic, Ras Bodik, Bryan Christopher Catanzaro, Joseph James Gebis, Parry Husbands, Kurt Keutzer, David A Patterson, William Lester Plishker, John Shalf, Samuel Webb Williams, and Katherine A Yelick. 2006. The landscape of parallel computing research: A view from Berkeley.
- [5] Brett W Bader and Tamara G Kolda. 2008. Efficient MATLAB computations with sparse and factored tensors. *SIAM Journal on Scientific Computing* 30, 1 (2008), 205–231.
- [6] Aart J. C. Bik and Harry A. G. Wijshoff. 1993. Compilation Techniques for Sparse Matrix Computations. In *International Conference on Supercomputing*. ACM, 416–424. <https://doi.org/10.1145/165939.166023>
- [7] Preston Briggs and Linda Torczon. 1993. An efficient representation for sparse sets. *ACM Letters on Programming Languages and Systems (LOPLAS)* 2, 1-4 (1993), 59–69.
- [8] Stephen Chou, Fredrik Kjolstad, and Saman Amarasinghe. 2018. Format Abstraction for Sparse Tensor Algebra Compilers. *Proc. ACM Program. Lang.* 2, OOPSLA, Article 123 (Oct. 2018), 30 pages.
- [9] Vidushi Dadu, Jian Weng, Sihao Liu, and Tony Nowatzki. 2019. Towards general purpose acceleration by exploiting common data-dependence forms. In *Proceedings of the 52nd Annual IEEE/ACM International Symposium on Microarchitecture*. 924–939.
- [10] Timothy A Davis and Yifan Hu. 2011. The University of Florida sparse matrix collection. *ACM Transactions on Mathematical Software (TOMS)* 38, 1 (2011), 1–25.
- [11] Evgeny Epifanovskiy, Michael Wormit, Tomasz Kuś, Arie Landau, Dmitry Zuev, Kirill Khistyayev, Prashant Manohar, Ilya Kaliman, Andreas Dreuw, and Anna I Krylov. 2013. New implementation of high-level correlated methods using a general block tensor library for high-performance electronic structure calculations.
- [12] Paul Grigoras, Pavel Burovskiy, Eddie Hung, and Wayne Luk. 2015. Accelerating SpMV in FPGAs by compressing nonzero values. In *2015 IEEE 23rd Annual International Symposium on Field-Programmable Custom Computing Machines*. IEEE, 64–67.
- [13] Song Han, Xingyu Liu, Huizi Mao, Jing Pu, Ardavan Pedram, Mark A Horowitz, and William J Dally. 2016. EIE: Efficient inference engine on compressed deep neural network. *ACM SIGARCH Computer Architecture News* 44, 3 (2016), 243–254.
- [14] Kartik Hegde, Hadi Asghari-Moghaddam, Michael Pellauer, Neal Crago, Aamer Jaleel, Edgar Solomonik, Joel Emer, and Christopher W Fletcher. 2019. Extensor: An accelerator for sparse tensor algebra. In *Proceedings of the 52nd Annual IEEE/ACM International Symposium on Microarchitecture*. 319–333.
- [15] Rawan Henry, Olivia Hsu, Rohan Yadav, Stephen Chou, Kunle Olukotun, Saman Amarasinghe, and Fredrik Kjolstad. 2021. Compilation of Sparse Array Programming Models. *Proc. ACM Program. Lang.* 5, OOPSLA, Article 128 (oct 2021), 29 pages. <https://doi.org/10.1145/3485505>
- [16] Yoongu Kim, Weikun Yang, and Onur Mutlu. 2016. Ramulator: A Fast and Extensible DRAM Simulator. *IEEE Comput. Archit. Lett.* 15, 1 (Jan. 2016), 45–49. <https://doi.org/10.1109/LCA.2015.2414456>
- [17] Fredrik Kjolstad, Peter Ahrens, Shoaib Kamil, and Saman Amarasinghe. 2019. Tensor Algebra Compilation with Workspaces. In *2019 IEEE/ACM International Symposium on Code Generation and Optimization (CGO)*. 180–192. <https://doi.org/10.1109/CGO.2019.8661185>
- [18] Fredrik Kjolstad, Shoaib Kamil, Stephen Chou, David Lugato, and Saman Amarasinghe. 2017. The tensor algebra compiler. *Proceedings of the ACM on Programming Languages* 1, OOPSLA (2017), 1–29.
- [19] Fredrik Berg Kjolstad. 2020. *Sparse tensor algebra compilation*. Ph.D. Dissertation. Massachusetts Institute of Technology.
- [20] David Koeplinger, Matthew Feldman, Raghu Prabhakar, Yaqi Zhang, Stefan Hadjis, Ruben Fiszal, Tian Zhao, Luigi Nardi, Ardavan Pedram, Christos Kozyrakis, and Kunle Olukotun. 2018. Spatial: A Language and Compiler for Application Accelerators. In *Proceedings of the 39th ACM SIGPLAN Conference on Programming Language Design and Implementation (Philadelphia, PA, USA) (PLDI 2018)*. Association for Computing Machinery, New York, NY, USA, 296–311. <https://doi.org/10.1145/3192366.3192379>
- [21] Vladimir Kotlyar, Keshav Pingali, and Paul Stodghill. 1997. A relational approach to the compilation of sparse matrix programs. In *Euro-Par Parallel Processing*. Springer, Passau, Germany, 318–327. <https://doi.org/10.1007/BFb0002751>
- [22] Tim Mattson, David Bader, Jon Berry, Aydin Buluc, Jack Dongarra, Christos Faloutsos, John Feo, John Gilbert, Joseph Gonzalez, Bruce Hendrickson, et al. 2013. Standards for graph algorithm primitives. In *2013 IEEE High Performance Extreme Computing Conference (HPEC)*. IEEE, 1–2.
- [23] Xinxin Mei and Xiaowen Chu. 2017. Dissecting GPU Memory Hierarchy Through Microbenchmarking. *IEEE Transactions on Parallel and Distributed Systems* 28, 1 (2017), 72–86. <https://doi.org/10.1109/TPDS.2016.2549523>
- [24] Ravi Teja Mullapudi, Andrew Adams, Dillon Sharlet, Jonathan Ragan-Kelley, and Kayvon Fatahalian. 2016. Automatically Scheduling Halide Image Processing Pipelines. *ACM Trans. Graph.* 35, 4, Article 83 (jul 2016), 11 pages. <https://doi.org/10.1145/2897824.2925952>
- [25] Subhankar Pal, Jonathan Beaumont, Dong-Hyeon Park, Apurva Amarath, Siying Feng, Chaitali Chakrabarti, Hun-Seok Kim, David Blaauw, Trevor Mudge, and Ronald Dreslinski. 2018. Outerspace: An outer product based sparse matrix multiplication accelerator. In *2018 IEEE International Symposium on High Performance Computer Architecture (HPCA)*. IEEE, 724–736.
- [26] Michael Pellauer, Yakun Sophia Shao, Jason Clemons, Neal Crago, Kartik Hegde, Rangharajan Venkatesan, Stephen W. Keckler, Christopher W. Fletcher, and Joel Emer. 2019. Buffets: An Efficient and Composable Storage Idiom for Explicit Decoupled Data Orchestration. In *Proceedings of the Twenty-Fourth International Conference on Architectural Support for Programming Languages and Operating Systems (Providence, RI, USA) (ASPLOS '19)*. Association for Computing Machinery, New York, NY, USA, 137–151. <https://doi.org/10.1145/3297858.3304025>
- [27] Raghu Prabhakar, Yaqi Zhang, David Koeplinger, Matt Feldman, Tian Zhao, Stefan Hadjis, Ardavan Pedram, Christos Kozyrakis, and Kunle Olukotun. 2017. Plasticine: A Reconfigurable Architecture For Parallel Patterns. *SIGARCH Comput. Archit. News* 45, 2 (June 2017), 389–402. <https://doi.org/10.1145/3140659.3080256>
- [28] Jonathan Ragan-Kelley, Andrew Adams, Sylvain Paris, Marc Levoy, Saman Amarasinghe, and Frédo Durand. 2012. Decoupling Algorithms from Schedules for Easy Optimization of Image Processing Pipelines. *ACM Trans. Graph.* 31, 4, Article 32 (July 2012), 12 pages. <https://doi.org/10.1145/2185520.2185528>

- [29] Jonathan Ragan-Kelley, Connelly Barnes, Andrew Adams, Sylvain Paris, Frédo Durand, and Saman Amarasinghe. 2013. Halide: A Language and Compiler for Optimizing Parallelism, Locality, and Recomputation in Image Processing Pipelines. In *Proceedings of the 34th ACM SIGPLAN Conference on Programming Language Design and Implementation* (Seattle, Washington, USA) (*PLDI '13*). Association for Computing Machinery, New York, NY, USA, 519–530. <https://doi.org/10.1145/2491956.2462176>
- [30] Alexander Rucker, Matthew Vilić, Tian Zhao, Yaqi Zhang, Raghu Prabhakar, and Kunle Olukotun. 2021. Capstan: A Vector RDA for Sparsity. In *MICRO-54: 54th Annual IEEE/ACM International Symposium on Microarchitecture* (Virtual Event, Greece) (*MICRO '21*). Association for Computing Machinery, New York, NY, USA, 1022–1035. <https://doi.org/10.1145/3466752.3480047>
- [31] Ryan Senanayake, Changwan Hong, Ziheng Wang, Amalee Wilson, Stephen Chou, Shoaib Kamil, Saman Amarasinghe, and Fredrik Kjolstad. 2020. A Sparse Iteration Space Transformation Framework for Sparse Tensor Algebra. *Proc. ACM Program. Lang.* 4, OOPSLA, Article 158 (Nov. 2020), 30 pages. <https://doi.org/10.1145/3428226>
- [32] Yi Shan, Tianji Wu, Yu Wang, Bo Wang, Zilong Wang, Ningyi Xu, and Huazhong Yang. 2010. FPGA and GPU implementation of large scale SpMV. In *2010 IEEE 8th Symposium on Application Specific Processors (SASP)*. IEEE, 64–70.
- [33] Nitish Srivastava, Hanchen Jin, Jie Liu, David Albonesi, and Zhiru Zhang. 2020. Matraport: A sparse-sparse matrix multiplication accelerator based on row-wise product. In *2020 53rd Annual IEEE/ACM International Symposium on Microarchitecture (MICRO)*. IEEE, 766–780.
- [34] Yaman Umuroglu and Magnus Jahre. 2014. An energy efficient column-major backend for FPGA SpMV accelerators. In *2014 IEEE 32nd International Conference on Computer Design (ICCD)*. IEEE, 432–439.
- [35] Anand Venkat, Mary Hall, and Michelle Strout. 2015. Loop and Data Transformations for Sparse Matrix Code. *SIGPLAN Not.* 50, 6 (June 2015), 521–532. <https://doi.org/10.1145/2813885.2738003>
- [36] Bimal Viswanath, Alan Mislove, Meeyoung Cha, and Krishna P Gummadi. 2009. On the evolution of user interaction in facebook. In *Proceedings of the 2nd ACM workshop on Online social networks*. 37–42.
- [37] Guowei Zhang, Nithya Attaluri, Joel S Emer, and Daniel Sanchez. 2021. Gamma: leveraging Gustavson’s algorithm to accelerate sparse matrix multiplication. In *Proceedings of the 26th ACM International Conference on Architectural Support for Programming Languages and Operating Systems*. 687–701.
- [38] Yaqi Zhang, Alexander Rucker, Matthew Vilić, Raghu Prabhakar, William Hwang, and Kunle Olukotun. 2019. Scalable Interconnects for Reconfigurable Spatial Architectures. In *2019 ACM/IEEE 46th Annual International Symposium on Computer Architecture (ISCA)*. 615–628.
- [39] Yan Zhang, Yasser H Shalabi, Rishabh Jain, Krishna K Nagar, and Jason D Bakos. 2009. FPGA vs. GPU for sparse matrix vector multiply. In *2009 International Conference on Field-Programmable Technology*. IEEE, 255–262.
- [40] Yaqi Zhang, Nathan Zhang, Tian Zhao, Matt Vilić, Muhammad Shahbaz, and Kunle Olukotun. 2021. SARA: Scaling a Reconfigurable Dataflow Accelerator. In *2021 ACM/IEEE 48th Annual International Symposium on Computer Architecture (ISCA)*. 1041–1054. <https://doi.org/10.1109/ISCA52012.2021.00085>
- [41] Zhekai Zhang, Hanrui Wang, Song Han, and William J Dally. 2020. Sparch: Efficient architecture for sparse matrix multiplication. In *2020 IEEE International Symposium on High Performance Computer Architecture (HPCA)*. IEEE, 261–274.
- [42] Tian Zhao, Yaqi Zhang, and Kunle Olukotun. 2019. Serving recurrent neural networks efficiently with a spatial accelerator. *arXiv preprint arXiv:1909.13654* (2019).